Advances in Engineering Materials, Structures and Systems: Innovations, Mechanics and Applications – Zingoni (Ed.)
© 2019 Taylor & Francis Group, London, ISBN 978-1-138-38696-9

Integrating structure and control design using tensegrity paradigm

Raman Goyal
Graduate Research Assistant, Department of Aerospace Engineering, Texas A&M University, College Station, TX, USA

Robert E. Skelton
TEES Distinguished Research Professor, Department of Aerospace Engineering, Texas A&M University, College Station, TX, USA

ABSTRACT: This paper provides a novel approach to jointly optimize structure parameters, information architecture (actuator/sensor precision) and control law to get the required system performance. The tensegrity paradigm is used to integrate these different yet interdependent fields. A linearized tensegrity model as an affine function of initial prestress and force density as the control input is developed. The optimal initial prestress in the strings; the assumed free structure parameter, is solved to satisfy performance and control energy upper bound. The precision of the sensors to measure the position and velocity of the nodes and the precision of actuators required to control the tension in the strings is also provided by the formulation. The complete problem is set as a covariance control problem where feasibility is achieved by bounding the covariance of the output as well as that of the control signals. The problem is formulated in the Linear Matrix Inequality (LMI) framework, and the feedback loop is assumed to have a full-order dynamic compensator with its characteristic matrices chosen as optimization variables. A sub-optimal solution of this non-convex system design problem is found by iterating over an approximated convex problem. The approximate problem is created using a convexifying potential function. This system-level optimization approach to design and control the tensegrity structures also provides the control law for the system.

1 INTRODUCTION

Traditionally structure design and control design have been treated as two separate problems where a structure is designed first, and then a control law is written to control the structure. It is only recently that researchers have realized the need for integrating the two disciplines. The idea is to design the structure and control algorithm to complement each other in achieving the required performance. Similarly, the knowledge of signal processing to locate the sensor/actuator and their respective precision should also be considered. Basically, a system level design approach is needed to make the best of all three disciplines. One such work was done by Li *et al.* who integrated Information Architecture (selection of sensor/actuator precision) and controller design by solving a covariance control problem (Li, de Oliveira, & Skelton 2008). Li *et al.* used the LMI (Linear Matrix Inequality) framework to show that the problem is convex and also provided a heuristic approach to locate the sensors and actuators. A linearly appearing free structure parameter was recently added to the above system design formulation (Goyal & Skelton 2019a). The contribution of this paper is to add prestress in the tensegrity structures as another dimension to this system design approach by integrating structure parameters as an optimization variable along with information architecture and controller design.

The authors believe that tensegrity structures are best suited to integrate structure and control design due to its very accurate models of axially loaded members (Goyal & Skelton 2019b). An accurate model of the system dynamics will yield precise control. Moreover, as tensegrity provides good efficiency for both structural and control avenue, it would be an ideal choice for various adaptive structures where structure and control parameters should be optimized simultaneously (Skelton & de Oliveira 2009). Tensegrity structures are defined as axially loaded rigid bodies arranged in a configuration that is stabilized by tension members (Fuller 1959, Snelson 1965). Skelton defined two types of tensegrity structures, where Class-1 represents the structure with at most one rigid body connected to a node, and Class-k structure contains a maximum of 'k' rigid bodies connected to a single node (Skelton & de Oliveira 2009). Tensegrity structures provide various prestressable self-equilibrium configurations for one particular topology. The different prestress values give different stiffness in the structure. Thus, one can change the stiffness of a tensegrity structure without changing the shape. Similarly, the shape

can also be changed without changing the stiffness. This property of tensegrity structures makes it robust to various kinds of loading conditions. These structures can be prestressed to have uni-directional loading for all the individual members giving the freedom to separately design tension and compression members. This freedom provides good structural efficiency (high strength to mass ratio) to tensegrity structures (Skelton & de Oliveira 2009). Tensegrity structures also require minimal control energy to change its shape as the structure will move from one equilibrium configuration to another equilibrium configuration (Karnan, Goyal, Majji, Skelton, & Singla 2017). All the above-mentioned properties of tensegrity structures have found their use in various applications ranging from bridges (Carpentieri, Skelton, & Fraternali 2015) in civil engineering to landers (SunSpiral, Gorospe, Bruce, Iscen, Korbel, Milam, Agogino, & Atkinson 2013, Goyal, Hernandez, & Skelton 2019), deployable structure (Tibert & Pellegrino 2003), and space habitats (Goyal, Bryant, Majji, Skelton, & Longman 2017) in aerospace engineering.

In this research work, we integrate structure, control and signal processing using tensegrity paradigm by framing it as a covariance control problem. A linearized tensegrity dynamics model with initial prestress as linearly appearing free structure parameter is developed. The model assumes force density in the strings to be the control input for the system. The performance is defined to bound the displacement of some nodes while measuring the length of the strings or the position of the nodes. The precision of the noisy actuators and sensors is also considered as an optimization variable. The cost of actuators and sensors is assumed to be directly proportional to their precision to add a budget constraint in the problem. Then, non-linear matrix inequalities are formulated to stabilize the system and bound the input and output performance (Skelton, Iwasaki, & Grigoriadis 1998). Convexifying LMI method is used to solve this system design problem by approximating it to a convex problem (Camino, de Oliveira, & Skelton 2003). The convexification is achieved by adding a non-linear matrix inequality with certain conditions. The iteration on the approximated convex sub-problem guarantees the solution to reach a stationary point. The final output of the optimization problem would be the initial prestress (free structure parameter), the precision of sensors/actuators, and the characteristics matrices for the dynamic controller. A 2-dimensional representation of a tensegrity lander is considered in the results section to show the effectiveness of the framework.

2 CONTROL FORMULATION

A continuous linear time-invariant system is described by the following *descriptor* state-space representation:

$$E(\alpha)\dot{x} = A(\alpha)x + Bu + D_p(\alpha)w_p + D_a(\alpha)w_a, \quad (1)$$

$$z = C_z x + D_s w_s, \quad y = C_y(\alpha)x, \quad (2)$$

where x is the state of the system, u is the control vector, z denotes the measurement vector, and y is the output of the system. The plant noise is denoted by w_p, and the sensor and actuator noise is denoted by w_s and w_a, respectively. These noises are modeled as independent zero mean white noises with intensities W_p, W_s, and W_a, respectively:

$$\mathcal{E}_\infty(w_i) = 0, \ \mathcal{E}_\infty(w_i w_i^\mathsf{T}) = W_i\delta(t-\tau), \quad (3)$$

where $i = a, s, p$, and $\mathcal{E}_\infty(x)$ denotes the asymptotic expected value of the random variable x. The vector α represents variable structure parameters that are assumed to be linear in plant matrices. The vectors γ_a and γ_s are defined to be precision of actuators and sensors, such that:

$$\mathrm{diag}(\gamma_a) \triangleq \Gamma_a \triangleq W_a^{-1}, \ \mathrm{diag}(\gamma_s) \triangleq \Gamma_s \triangleq W_s^{-1}. \quad (4)$$

A total design price is also added as:

$$\$ = p_a^\mathsf{T}\gamma_a + p_s^\mathsf{T}\gamma_s + p_\alpha^\mathsf{T}\alpha, \quad (5)$$

where p_a, p_s and p_α are vectors containing the price per unit of actuator precision, sensor precision and price per unit of structure parameter, respectively.

Theorem 2.1. Let a continuous time-invariant linear system be described by equations (1–2). There exist controller matrices A_c, B_c, C_c, structure parameters α, and precisions γ_a, γ_s such that the input and output performance constraints $(\mathcal{E}_\infty(uu^\mathsf{T}) \prec \bar{U}, \mathcal{E}_\infty(yy^\mathsf{T}) \prec \bar{Y})$ are satisfied, if and only if for some constant matrix G, there exists a symmetric matrix Q, such that the following *LMIs* are satisfied:

$$p_a^\mathsf{T}\gamma_a + p_s^\mathsf{T}\gamma_s + p_\alpha^\mathsf{T}\alpha < \bar{\$} \quad (6)$$

$$\gamma_a < \bar{\gamma}_a, \quad \gamma_s < \bar{\gamma}_s, \quad \bar{\alpha}_L < \alpha < \bar{\alpha}_U \quad (7)$$

$$\begin{bmatrix} \bar{U} & M_{cl} \\ M_{cl}^\mathsf{T} & Q \end{bmatrix} \succ 0, \quad \begin{bmatrix} \bar{Y} & C_{cl} \\ C_{cl}^\mathsf{T} & Q \end{bmatrix} \succ 0 \quad (8)$$

$$\begin{bmatrix} (\star) & B_{cl} & A_{cl} & E_{cl} \\ B_{cl}^\mathsf{T} & -W^{-1} & 0 & 0 \\ A_{cl}^\mathsf{T} & 0 & -Q & 0 \\ E_{cl}^\mathsf{T} & 0 & 0 & -Q \end{bmatrix} \prec 0 \quad (9)$$

where

$$(\star) = -(A_{cl} - E_{cl})G^\mathsf{T} - G(A_{cl} - E_{cl})^\mathsf{T} + GQG^\mathsf{T},$$

$$W = \begin{bmatrix} W_p & 0 & 0 \\ 0 & W_a & 0 \\ 0 & 0 & W_s \end{bmatrix}, \quad A_{cl} = \begin{bmatrix} A(\alpha) & BC_c \\ B_cC_z & A_c \end{bmatrix},$$

$$E_{cl} = \begin{bmatrix} E(\alpha) & 0 \\ 0 & I_n \end{bmatrix}, B_{cl} = \begin{bmatrix} D_p(\alpha) & D_a(\alpha) & 0 \\ 0 & 0 & B_cD_s \end{bmatrix},$$

$$C_{cl} = \begin{bmatrix} C_y(\alpha) & 0 \end{bmatrix}, \quad M_{cl} = \begin{bmatrix} 0 & C_c \end{bmatrix},$$

and I_n is a $n \times n$ identity matrix.

Proof. Let us write the controller of the form:

$$\dot{x}_c = A_c x_c + B_c z, \quad u = C_c x_c, \tag{10}$$

which can be used to write the closed loop dynamics in the state $\tilde{x}$ as $\tilde{x}^\mathsf{T} = \begin{bmatrix} x^\mathsf{T} & x_c^\mathsf{T} \end{bmatrix}$ and noise vector w as $w^\mathsf{T} = \begin{bmatrix} w_p^\mathsf{T} & w_a^\mathsf{T} & w_s^\mathsf{T} \end{bmatrix}$ as:

$$E_{cl}\dot{\tilde{x}} = A_{cl}\tilde{x} + B_{cl}w, \tag{11}$$

$$y = C_{cl}\tilde{x}, \quad u = M_{cl}\tilde{x} + F_{cl}w. \tag{12}$$

The standard result for stability of closed loop system for a positive definite symmetric matrix ($X \succ 0$) is:

$$A_{cl}XE_{cl}^\mathsf{T} + E_{cl}XA_{cl}^\mathsf{T} + B_{cl}WB_{cl}^\mathsf{T} \prec 0. \tag{13}$$

After applying multiple Schur's complements and manipulations, we can write the above inequality as:

$$\mathcal{F}(\delta) \triangleq \begin{bmatrix} (\bullet) & B_{cl} & A_{cl} & E_{cl} \\ B_{cl}^\mathsf{T} & -W^{-1} & 0 & 0 \\ A_{cl}^\mathsf{T} & 0 & -Q & 0 \\ E_{cl}^\mathsf{T} & 0 & 0 & -Q \end{bmatrix} \prec 0,$$

where $\delta \triangleq (A_c, B_c, C_c, \gamma_a, \gamma_s, \alpha, Q)$, $Q \triangleq X^{-1}$, and $(\bullet) = -(A_{cl} - E_{cl})X(A_{cl} - E_{cl})^\mathsf{T}$. Note that $\mathcal{F}(\delta)$ is not an LMI. Please refer (Camino, de Oliveira, & Skelton 2003) for **Convexifying Algorithm Lemma** to write a new LMI.

To use the **Convexifying Algorithm Lemma**, let us define the matrix G as:

$$G(\eta) \triangleq (A_{cl} - E_{cl})X \tag{14}$$

and the convexifying potential function as:

$$\mathcal{G}(\delta, \eta) \triangleq \begin{bmatrix} (*) & \mathbf{0} \\ \mathbf{0} & \mathbf{0} \end{bmatrix} \succeq 0$$

$$(*) = (A_{cl} - E_{cl} - G(\eta)Q)X(A_{cl} - E_{cl} - G(\eta)Q)^\mathsf{T}$$

The matrix function $\mathcal{F}(\delta) + \mathcal{G}(\delta, \eta)$:

$$\begin{bmatrix} (\star) & B_{cl} & A_{cl} & E_{cl} \\ B_{cl}^\mathsf{T} & -W^{-1} & 0 & 0 \\ A_{cl}^\mathsf{T} & 0 & -Q & 0 \\ E_{cl}^\mathsf{T} & 0 & 0 & -Q \end{bmatrix} < 0, \tag{15}$$

where $(\star) = -(A_{cl} - E_{cl})G^\mathsf{T} - G(A_{cl} - E_{cl})^\mathsf{T} + GQG^\mathsf{T}$, is convex, where the dependency of the matrix G on η is omitted for brevity. The other LMIs can easily be derived as:

$$\mathcal{E}_\infty(uu^\mathsf{T}) < \bar{U} \Rightarrow M_{cl}XM_{cl}^\mathsf{T} < \bar{U}, \tag{16}$$

$$\mathcal{E}_\infty(yy^\mathsf{T}) < \bar{Y} \Rightarrow C_{cl}XC_{cl}^\mathsf{T} < \bar{Y}. \tag{17}$$

The more detailed proof of this theorem can be found in (Goyal & Skelton 2019a).

Algorithm for the Optimum Solution Let one parameter out of the set ($\bar{\$}, \bar{U}, \bar{Y}$) be the optimization variable $\bar{f}$. The following iterative algorithm takes advantage of Convexifying Lemma to find a minimum for $\bar{f}$.

- Set fixed nominal values for α_0. Compute controller matrices $A_{c,0}$, $B_{c,0}$, $C_{c,0}$, precision vectors $\gamma_{a,0}$, $\gamma_{s,0}$ and state covariance matrix X_0 according to (Li, de Oliveira, & Skelton 2008) or some alternative method. Set ϵ to some prescribed tolerance and $i = 0$
- **Repeat:** Set $G_i \leftarrow (A_{cl}(\alpha_i) - E_{cl}(\alpha_i))X_i$
  - For fixed $G = G_i$, find the extrema of $\bar{f}$ for which the LMIs of Theorem 2.1 are feasible
  - Denote the solution ($\bar{f}_{i+1}$, α_{i+1}, $A_{c,i+1}$, $B_{c,i+1}$, $C_{c,i+1}$,$\gamma_{a,i+1}$, $\gamma_{s,i+1}$,X_{i+1})
  - Set $i = i + 1$
- **Until:** $\|\bar{z}_i - \bar{z}_{i-1}\| < \epsilon$

3 LINEARIZED TENSEGRITY DYNAMICS

The nonlinear dynamics of a tensegrity structure of any complexity is derived in (Goyal & Skelton 2019b). To apply the optimization in Section 2, the nonlinear equations are linearized and represented in the descriptor form such that prestress appears as a linear free variable. The vector equations for rotational dynamics of a bar can be written as:

$$J_1\ddot{b}_1 + \frac{J_1}{l_1^2}b_1\dot{b}_1^\mathsf{T}\dot{b}_1 = \frac{1}{2}(f_2 - f_1) - \frac{1}{2l_1^2}b_1b_1^\mathsf{T}(f_2 - f_1),$$

where b_1 and $\dot{b}_1$ represent the bar vector (length l_1) and bar velocity vector respectively. f_1 and f_2 represent the total forces on both ends of the bar and $J_1 = m_1/12$, which comes from a consideration of the moment of inertia of the bar of mass m_1. The translational dynamics with r_1 being the position vector of the center of mass of the bar can be written as:

$$m_1\ddot{r}_1 = f_1 + f_2, \tag{18}$$

and the equation for a point mass (connecting string to string node) is given as:

$$m_{s1}\ddot{r}_{s1} = f_3. \tag{19}$$

These vector equations can be combined for any number of bars and point masses to form a matrix second-order differential equation that defines the non-linear dynamics of any tensegrity system:

$$\ddot{N}M + NK = W. \tag{20}$$

Please refer to (Goyal & Skelton 2019b) for the definitions of matrix variables in equation (20).

To use the optimization algorithm of Section 2, the nonlinear tensegrity dynamics can be linearized according to the following lemmas.

Lemma 3.1. The linearized dynamics of any class-1 tensegrity system in terms of linear variation in nodal coordinates $\tilde{n}$ can be written as:

$$\mathcal{M}\ddot{\tilde{n}} + \mathcal{D}\dot{\tilde{n}} + \mathcal{K}\tilde{n} = \mathcal{F}\tilde{w} + \mathcal{B}\tilde{\gamma}, \tag{21}$$

where $\tilde{\gamma}$ is the linear variation in the force density, $\tilde{w}$ is the linear variation in external force, and

$$\mathcal{M} \triangleq \mathcal{T}^{\mathsf{T}} M_{br} \mathcal{T},\ \mathcal{D} \triangleq \mathcal{T}^{\mathsf{T}} D_{br} \mathcal{T},$$

$$\mathcal{K} \triangleq \mathcal{T}^{\mathsf{T}} K_{br} \mathcal{T} + \mathcal{T}^{\mathsf{T}} P_{br} \left(C_s^{\mathsf{T}} \otimes I\right) \widehat{(\bar{\gamma} \otimes \mathbb{1})} \left(C_s \otimes I\right),$$

$$\mathcal{F} \triangleq \mathcal{T}^{\mathsf{T}} P_{br},\ \mathcal{B} \triangleq -\mathcal{T}^{\mathsf{T}} P_{br} (C_s^{\mathsf{T}} \otimes I)\hat{\bar{s}},$$

$$\mathcal{T} \triangleq \left(\begin{bmatrix} C_b \\ C_r \\ C_{ns} \end{bmatrix} \otimes I \right),$$

where $\mathbb{1} \triangleq [1\ \ 1\ \ 1]^{\mathsf{T}}$ with C_b, C_s, C_r and C_{ns} being the connectivity matrices for bars, strings, center of the bars and point masses, respectively. The matrices $M_{br} \triangleq blkdiag(M_b, M_r, M_{rs})$, $D_{br} \triangleq blkdiag(D_b, \mathbf{0}, \mathbf{0})$, and $K_{br} \triangleq blkdiag(K_b, \mathbf{0}, \mathbf{0})$ are block diagonal matrices with $M_b \triangleq diag(J_1 I, J_2 I, \dots)$, $M_r \triangleq diag(m_1 I, m_2 I, \dots)$, $M_{rs} \triangleq diag(m_{s1} I, m_{s2} I, \dots)$, $D_b \triangleq diag(D_{b1}, D_{b2}, \dots)$, and $K_b \triangleq diag(K_{b1}, K_{b2}, \dots)$.

$$P_{br} \triangleq \begin{bmatrix} P_b & \mathbf{0} \\ P_r & \mathbf{0} \\ \mathbf{0} & I \end{bmatrix},\ D_{b1} \triangleq \frac{2J_1}{\bar{l}_1^2} \bar{b}_1 \dot{\bar{b}}_1^{\mathsf{T}},$$

$$K_{b1} \triangleq \left[\frac{J_1}{\bar{l}_1^2} \dot{\bar{b}}_1^{\mathsf{T}} \dot{\bar{b}}_1 + \frac{1}{2\bar{l}_1^2} \bar{b}_1^{\mathsf{T}} (\bar{f}_2 - \bar{f}_1) \right] I + \frac{1}{2\bar{l}_1^2} \bar{b}_1 (\bar{f}_2 - \bar{f}_1)^{\mathsf{T}},$$

$$P_{r1} \triangleq [I\ I],\ P_{b1} \triangleq \frac{1}{2} \left(I - \frac{\bar{b}_1 \bar{b}_1^{\mathsf{T}}}{\bar{l}_1^2} \right) [-I\ I],$$

where $P_b \triangleq diag(P_{b1}, P_{b2}, \dots)$, and $P_r \triangleq diag(P_{r1}, P_{r2}, \dots)$ with bar vector $\bar{b}_1$, string vector $\bar{s}_1$, bar velocity vector $\dot{\bar{b}}_1$, center of mass vector $\bar{r}_1$, center of mass velocity vector $\dot{\bar{r}}_1$, point mass vector $\bar{r}_{s1}$ and force $\bar{f}$, represents the vectors about which the dynamics is linearized.

Lemma 3.2. The reduced-order linearized dynamics of any class-k tensegrity system can be written as:

$$\mathcal{M}_k \ddot{\tilde{\eta}}_2 + \mathcal{D}_k \dot{\tilde{\eta}}_2 + \mathcal{K}_k \tilde{\eta}_2 = \mathcal{F}_k \tilde{w} + \mathcal{B}_k \tilde{\gamma}, \tag{22}$$

where $\mathcal{M}_k \triangleq V_2^{\mathsf{T}} \mathcal{M} V_2, \mathcal{D}_k \triangleq V_2^{\mathsf{T}} \mathcal{D} V_2, \mathcal{K}_k \triangleq V_2^{\mathsf{T}} \mathcal{K} V_2$, $\mathcal{F}_k \triangleq V_2^{\mathsf{T}} \mathcal{F}, \mathcal{B}_k \triangleq V_2^{\mathsf{T}} \mathcal{B}$, with some linear constraints of the form for class-k structure as:

$$A\tilde{n} = 0,\ U \begin{bmatrix} \Sigma_1 & 0 \end{bmatrix} \begin{bmatrix} V_1^{\mathsf{T}} \\ V_2^{\mathsf{T}} \end{bmatrix} \tilde{n} = U \begin{bmatrix} \Sigma_1 & 0 \end{bmatrix} \begin{bmatrix} \tilde{\eta}_1 \\ \tilde{\eta}_2 \end{bmatrix} = 0,$$

implying $\tilde{\eta}_1 = \dot{\tilde{\eta}}_1 = \ddot{\tilde{\eta}}_1 = 0$.

Equation (22) for a class-k tensegrity structure can be represented in the following descriptor form:

$$\begin{bmatrix} I & 0 \\ 0 & \mathcal{M}_k \end{bmatrix} \begin{bmatrix} \dot{\eta}_2 \\ \ddot{\eta}_2 \end{bmatrix} = \begin{bmatrix} 0 & I \\ -\mathcal{K}_k & -\mathcal{D}_k \end{bmatrix} \begin{bmatrix} \eta_2 \\ \dot{\eta}_2 \end{bmatrix} + \begin{bmatrix} 0 \\ \mathcal{F}_k \end{bmatrix} w + \begin{bmatrix} 0 \\ \mathcal{B}_k \end{bmatrix} \gamma + \begin{bmatrix} 0 \\ \mathcal{B}_k \end{bmatrix} w_a. \tag{23}$$

Notice that the tildes above the dynamics variables have been removed assuming small linear variations around the equilibrium condition. Equation (23) can also represent class-1 dynamics when the subscript 'k' is omitted from $\mathcal{M}_k, \mathcal{D}_k, \mathcal{K}_k, \mathcal{B}_k, \mathcal{F}_k$, and $\tilde{\eta}_2$ is replaced by $\tilde{n}$.

In this problem formulation, we define the control input to be force density in the strings ($u = \gamma$), process noise to be ($w_p = w$), actuator noise to be w_a (same coefficient matrix), and structure parameter to be initial prestress or force density at equilibrium condition ($\alpha = \bar{\gamma}$). It is to be noted that $\mathcal{K}_k(\bar{\gamma})$ is affine in initial prestress value $\bar{\gamma}$ as:

$$\mathcal{K}_k(\bar{\gamma}) = V_2^{\mathsf{T}} \mathcal{T}^{\mathsf{T}} P_{br} \left(C_s^{\mathsf{T}} \otimes I\right) \widehat{(\bar{\gamma} \otimes \mathbb{1})} \left(C_s \otimes I\right) V_2^{\mathsf{T}} + V_2^{\mathsf{T}} \mathcal{T}^{\mathsf{T}} K_{br}(\bar{f}, \bar{b}, \dot{\bar{b}}) \mathcal{T} V_2, \tag{24}$$

where $K_{br}(\bar{f}, \bar{b}, \dot{\bar{b}})$ can also be written as some affine function of $\bar{\gamma}$ as $K_{br}(\bar{f}, \bar{b}, \dot{\bar{b}}) = \mathcal{G}\bar{\gamma}$. Comparing it to system equation (1), we see only system matrix $A(\alpha)$ to be dependent on structure parameter.

4 TENSEGRITY EXAMPLE

For a given 2D tensegrity structure shown in Figure 1, this section optimizes the optimal pre-stresses in each string, precisions of sensors and actuators, and matrices corresponding to the dynamic controller for covariance control. The bars are shown in black, and the strings are shown in red. The example is inspired by a tensegrity lander where the point mass (node 5) is the payload to capture the images, and the two bars are fixed to ground depicting the lander in the landed position.

The mass for both the bars are assumed to be $m_b = 1$ Kg and the mass for point mass is assumed to be $m_s = 0.5$ Kg. The tensegrity dynamics is linearized about the equilibrium configuration (corresponding to Figure 1) with prestress values of $\alpha_0 = \bar{\gamma} = [1, 2.76, 1, 1, 1, 1, 1]^{\mathsf{T}}$ and no external force. The disturbances come from the external force which is modeled as a zero-mean white noise with intensity $W_p = 1\ \mathrm{N}^2$. The disturbances are present only on nodes 2, 3, and 5. All seven strings are actuated to control the

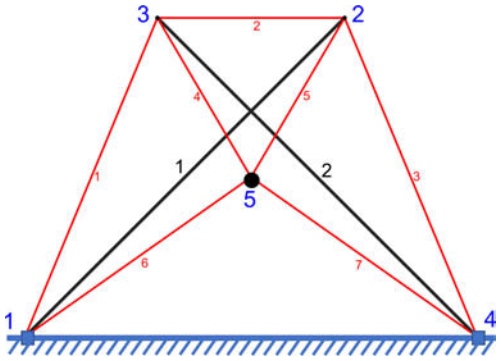

Figure 1. 2D Tensegrity Lander.

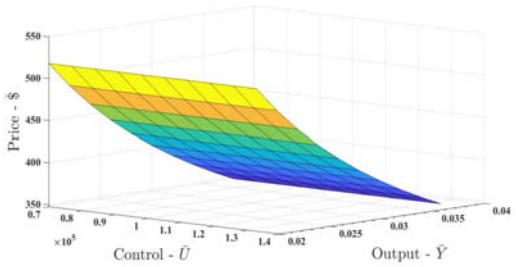

Figure 2. A surface plot of the variation in budget with input-$\bar{U}$ and output-$\bar{Y}$.

structure. The output to be bound is the displacement of payload (node 5) in x and y-direction.

$$y = \begin{bmatrix} n_{5x} \\ n_{5y} \end{bmatrix} = C_y \begin{bmatrix} \eta_2 \\ \dot{\eta}_2 \end{bmatrix}, \; C_y = [0 \quad I]\, V_2\, [I \quad 0], \quad (25)$$

and the measurements are the positions and velocity of nodes 2, 3, and 5 (nodes 1 and 4 are fixed to ground).

$$z = C_z \begin{bmatrix} \eta_2 \\ \dot{\eta}_2 \end{bmatrix} + I w_s, \; C_z = \begin{bmatrix} V_2 & 0 \\ 0 & V_2 \end{bmatrix}. \quad (26)$$

Some values assumed for this example are $\bar{\alpha}_L = 0.1\alpha_0$, $\bar{\alpha}_U = 10\alpha_0$, $\bar{\gamma}_a = \bar{\gamma}_s = 1e3, p_a = p_s = 2$, and $p_\alpha = 10$.

The surface plot in Figure 2 shows the variation in budget requirement $ as we change the input covariance bound $\bar{U}$ and output covariance bound $\bar{Y}$. The required budget monotonically decreases with more relaxed performance constraint for all values of control input bounds. The same decreasing trend in budget follows as we increase the control input bound. This variation is small showing the relatively less strict nature of control covariance bound.

Figure 3(a) shows the decreasing variation in the prestress required for all strings as we increase the output covariance bound while maintaining the same control input $\bar{U}$. Basically, less prestress is required for relaxed performance constraint. The result shows that strings 1 and 3 have the same prestress values and variations. This can be understood from the symmetry

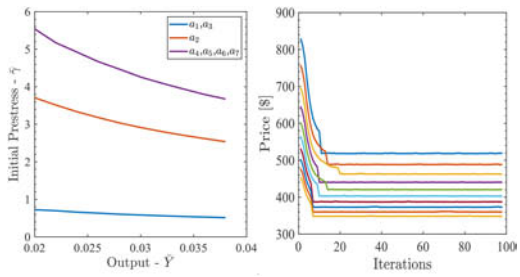

Figure 3. (a)Variation in the optimal prestress with $\bar{Y}$. (b) Convergence of minimum price required. $\bar{U} = 10^4\,\mathrm{N}^2/\mathrm{m}^2$ for all 7 strings.

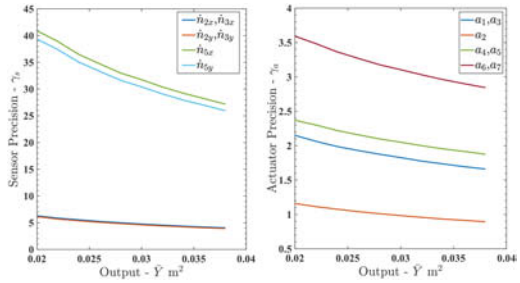

Figure 4. (a)Variation in the required sensor precision. (b) Variation in the required actuator precision.

of the structure. Similarly, strings 4, 5, 6, and 7 follow the same trend. Notice that the optimization requires strings 4, 5, 6, and 7 to have high prestress value as these strings are directly connected to the payload. Figure 3(b) shows the effectiveness of the algorithm as the price converges in about 20 to 30 iterations. The 10 different lines in the plot represent different values of performance constraints $\bar{Y}$ =(0.02 m^2 to 0.04 m^2).

The variation in required sensor precision with varying output bound $\bar{Y}$ is shown in Figure 4(a). The sensors corresponding to $\dot{n}_{2x}$ and $\dot{n}_{3x}$ overlaps because of symmetry. Similarly, $\dot{n}_{2y}$ and $\dot{n}_{3y}$ overlaps. As the output to be bounded is the displacement of node 5 in x and y-direction, higher precision is required for $\dot{n}_{5x}$ and $\dot{n}_{5y}$. The figure shows that less precision on sensors and actuators is required for relaxed performance requirement. Figure 4(b) shows that more precision is required on strings 4, 5, 6, and 7 as these strings are directly connected to the payload.

5 CONCLUSION

This paper uses the tensegrity paradigm to integrate the structure and control design along with the information architecture. A linearized tensegrity dynamics model was developed with initial prestress in the strings as a free structure parameter which appears linearly in the system matrices. The force density in the strings is used as the control input. The precision of the sensors and actuators is also considered as the

optimization variable. A dynamic controller is generated to bound the covariance of inputs and outputs. The covariance control problem is formulated in the LMI framework where the combined optimization for structure parameter, sensor/actuator precision, and control law was found to be a non-convex problem. The nonlinear matrix inequalities constraints were approximated as linear matrix inequalities by adding a convexifying potential function. A stationary solution was achieved by iterating over the approximated convex problem. A 2-dimensional tensegrity lander topology was used as an example to show the effectiveness of the developed results. The example results provide the knowledge on price estimate, what initial prestress to choose, where to put more precise sensors/actuators and the controller parameters.

REFERENCES

Camino, J. F., M. de Oliveira, & R. Skelton (2003, July). Convexifying Linear Matrix Inequality Methods for Integrating Structure and Control Design. *Journal of Structural Engineering Vol.129*(No.7).

Carpentieri, G., R. E. Skelton, & F. Fraternali (2015). Minimum mass and optimal complexity of planar tensegrity bridges. *International Journal of Space Structures 30* (3–4), 221–243.

Fuller, R. B. (1959). Tensile integrity structures. US Patent 3.063.521.

Goyal, R., T. Bryant, M. Majji, R. E. Skelton, & A. Longman (2017). Design and control of growth adaptable artificial gravity space habitat. In *AIAA SPACE and Astronautics Forum and Exposition*, pp. 5141.

Goyal, R., E. A. P. Hernandez, & R. E. Skelton (2019). Analytical study of tensegrity lattices for mass-efficient mechanical energy absorption. *International Journal of Space Structures*.

Goyal, R. & R. E. Skelton (2019a). Joint optimization of plant, controller, and sensor/actuator design. In *American Control Conference, Philadelphia, USA, July 10–12*.

Goyal, R. & R. E. Skelton (2019b). Tensegrity system dynamics with rigid bars and massive strings. *Multibody System Dynamics* 1–26.

Karnan, H., R. Goyal, M. Majji, R. E. Skelton, & P Singla (2017, Sept). Visual feedback control of tensegrity robotic systems. *2017 IEEE/RSJ-IROS* 2048–2053.

Li, F., M. C. de Oliveira, & R. E. Skelton (2008, March). Integrating Information Architecture and Control or Estimation Design. *SICE Journal of Control, Measurement, and System Integration Vol.1* (No.2).

Skelton, R. E. & M. C. de Oliveira (2009). *Tensegrity Systems* Springer US.

Skelton, R. E., T. Iwasaki, & K. Grigoriadis (1998). *A Unified Algebraic Approach to Control Design.* Taylor & Francis, London, UK.

Snelson, K. D. (1965, February 16). Continuous tension, discontinuous compression structures. US Patent 3,169,611.

SunSpiral, V., G. Gorospe, J. Bruce, A. Iscen, G. Korbel, S. Milam, A. Agogino, & D. Atkinson (2013). Tensegrity based probes for planetary exploration: Entry descent and landing (EDL) and surface mobility analysis. *International Journal of Planetary Probes 7*.

Tibert, A. G. & S. Pellegrino (2003). Deployable tensegrity mast. *In: 44th AIAA/ASME/ASCE, Structures, Structural Dynamics and Materials Conference and Exhibit, Norfolk VA, USA.* 1978.